Journal of Polyphenols
2026, 8 (1): 53–62
journal homepage: http://jpolyph.magtechjournal.com

Protective effect of procyanidin B2-3′-*O*-gallate on ulcerative colitis in mice

Mingyu Sun [1], Peiyan Han [1], Jiao Fang [1], Yan Han [1], Li Ma [1], Shuting Zhang [1*], Baoshan Sun [1,2*]

1. Faculty of Functional Food and Wine, Shenyang Pharmaceutical University, Shenyang 110016, China;
2. Pólo de Inovação de Dois Portos, Instituto Nacional de Investigação Agrária e Veterinária, I.P., Quinta da Almoinha, 2565-191 Dois Portos, Portugal

Abstract Ulcerative colitis (UC) is a globally prevalent disease with a continuously increasing incidence rate. Galloylated procyanidins (GPCs) are promising polyphenols for UC treatment. In this study, the protective effects of B2-3′-*O*-gallate (B2-3′-G), a typical GPC derived from grape seeds, were explored for the first time using a dextran sulfate sodium (DSS)-induced colitis mouse model. Treatment with B2-3′-G obviously mitigated body weight loss and reduced the Disease Activity Index (DAI). DSS-triggered splenomegaly and colonic shortening were also relieved after B2-3′-G administration. Hematoxylin and eosin (H&E) staining results indicated that B2-3′-G preserved the integrity of colonic mucosa, restored crypt morphology and inhibited inflammatory cell infiltration. Alcian Blue/Periodic Acid-Schiff (AB-PAS) staining further showed that B2-3′-G treatment increased the number of goblet cells, enhanced mucus secretion, and improved the continuity and thickness of the intestinal mucus layer. Collectively, these results confirm that B2-3′-G alleviates DSS-induced colitis by reducing intestinal inflammation and restoring colonic barrier function.

Keywords: Galloylated procyanidins; B2-3′-*O*-gallate; Ulcerative colitis

1 Introduction

Inflammatory bowel disease (IBD) is a chronic recurrent inflammatory disorder affecting the gastrointestinal tract, characterized by mucosal ulceration, rectal bleeding, diarrhea, and body weight loss, and the main clinical subtypes are ulcerative colitis (UC) and Crohn's disease [1]. The prevalence of UC reaches 1.0%, while that of Crohn's disease is 0.3%. UC also presents a higher incidence of complications and more severe clinical symptoms compared with Crohn's disease [2], and long-term UC may progress to colon cancer [3]. At present, major clinical drugs for UC include sulfasalazine, 5-aminosalicylic acid, steroids, hormones, and immunosuppressants. Nevertheless, these drugs show limited efficacy in repairing damaged intestinal barriers and are accompanied by obvious side effects [4]. Natural polyphenolic compounds derived from natural sources have attracted widespread attention due to their diverse biological functions and high safety.

Proanthocyanidins (PAs) are a large group of natural polyphenols widely distributed in plants such as grape seeds. These compounds possess potent antioxidant and anti-inflammatory properties [5]. Existing studies have verified that PAs exert protective effects against UC through inhibiting inflammatory responses, alleviating oxidative stress, repairing intestinal mucosal barriers and regulating intestinal

* Corresponding author: zstsyphu@163.com; sun.baoshan@iniav.pt.
These authors have no conflict of interest to declare.

microbiota [6-8].

The biological activities of PAs are closely associated with their specific functional groups. Modification to form galloylated proanthocyanidins (GPCs) can markedly enhance the bioactivity of PAs. Given their superior biological [9-10] performance, GPCs exhibit great potential for the development of novel anti-UC agents.

Despite strong bioactivity, natural GPCs exist at extremely low concentrations and possess complex structures characterized by stereoisomerism and structural polymerization. The relatively more abundant B2-3′-*O*-gallate (B2-3′-G) account for less than 0.5% of grape seed procyanidins [9]. Traditional isolation techniques cannot achieve efficient preparation of B2-3′-G, and large-scale production remains challenging. Consequently, the biological activities of B2-3′-G remain largely unexplored.

The present work aims to clarify the protective effects of B2-3′-G against UC. A DSS-induced UC mouse model was established, and the efficacy of B2-3′-G was evaluated by detecting changes in body weight, DAI scores, colon length, spleen index and histopathological characteristics. The findings provide experimental evidence for revealing the action mechanism of B2-3′-G against UC and support the development of new therapeutic strategies for this disease.

2 Materials and methods

2.1 Materials

Dextran sulfate sodium (DSS, molecular weight: 40 kDa) was purchased from Shanghai Macklin Biochemical Co., Ltd., Shanghai, China. Fecal occult blood detection kits were obtained from Beijing Solarbio Science & Technology Co., Ltd., (Beijing, China. Hematoxylin and eosin (H&E) staining reagents and Alcian Blue/Periodic Acid-Schiff (AB-PAS) staining kits were supplied by Wuhan Servicebio Technology Co., Ltd., Wuhan, China. Distilled water was purchased from Hangzhou Wahaha Group Co., Ltd., Hangzhou, China. All organic solvents were acquired from the Chemical Branch of Shandong Yuwang Industrial Co., Ltd., Shandong, China. Procyanidin B2, epicatechin-3-*O*-gallate (ECG), epicatechin (EC) and gallic acid (GA) were provided by Chengdu Must Bio-Technology Co., Ltd., Chengdu, China. Grape seed extract was obtained from Tianjin Jianfeng Natural Product R&D Co., Ltd., Tianjin, China. L-Cysteine and citric acid were purchased from Shanghai Aladdin Biochemical Technology Co., Ltd., Shanghai, China.

2.2 Preparation of polymeric procyanidins (PPCs)

Grape seeds were separated from white grape pomace, dried at a temperature below 40 °C for 24 h in a ventilated environment, sealed under nitrogen atmosphere and stored at -20 °C. The seeds were ground into powder with liquid nitrogen before use. Grape seed powder was extracted separately with 80% methanol aqueous solution and 75% acetone aqueous solution. Each extraction was performed under nitrogen protection for 3 h. All extraction solutions were combined, and organic solvents were removed by evaporation. Lipid components were eliminated via extraction with *n*-hexane, and the aqueous phase was freeze-dried to obtain crude total polyphenol extracts. High-speed counter-current chromatography (HSCCC) was applied for further separation. The two-phase solvent system consisted of *n*-hexane-ethyl acetate-water at a volume ratio of 1:50:50. The lower phase served as the stationary phase and the upper phase as the mobile phase. A total of 400 mg of crude grape seed procyanidin extract was separated in tail-to-head elution mode at a flow rate of 3.0 mL/min, a rotational speed of 950 rpm and a constant temperature of 25 °C [11].

2.3 Preparation of epicatechin-3-O-gallate (ECG)

Epicatechin-3-*O*-gallate (ECG) was further isolated from 200 mg of fraction F1 using HSCCC based on the above PPC preparation method. The solvent system was n-hexane-ethyl acetate-water (1:10:10, v/v/v), and dual-direction elution including head-to-tail and tail-to-head dual-direction modes was adopted [11].

2.4 Preparation of B2-3'-G

Nucleophilic degradation of PPCs using L-cysteine [12]. PPCs (1 g), citric acid (1 g), and L-cysteine (Cys, 3 g) were dissolved in 50 mL of distilled water. The mixed solution was incubated at 75 °C for 5.6 h in a reaction tube, and the reaction was terminated immediately by an ice bath at 0 °C. The mixture was diluted with distilled water and freeze-dried. Crude oligomeric procyanidins (OPCs) were collected after liquid–liquid extraction. The lyophilized degradation products were re-dissolved in distilled water and extracted three times with 400 mL of ethyl acetate. The organic phase was combined and evaporated to dryness under vacuum at a temperature lower than 35 °C. Purification was performed using a Shimadzu semi-preparative high-performance liquid chromatography (HPLC) system equipped with a YMC-Pack ODS-A C_{18} column (10 mm × 250 mm, 5 μm). The column temperature was set at 30 °C, and the detection wavelength was 280 nm. The mobile phase consisted of water (solvent A) and methanol (solvent B), and isocratic elution was conducted with 20% solvent B at a flow rate of 3.5 mL/min.

Semi-synthesis with ECG [13]. PPCs (200 mg) and ECG (600 mg) were dissolved in 50 mL of 0.1 M methanolic HCl. The mixture was transferred to a stoppered test tube and incubated at 55 °C with shaking for 1.5 h. The reaction was terminated by an ice bath for 10 min. Methanol was removed by rotary evaporation at 35 °C. The residual product was dissolved in distilled water and extracted three times with 400 mL of ethyl acetate. All organic fractions were combined and dried at 35 °C. Crude products were purified using a Shimadzu LC-20AR semi-preparative HPLC system with a YMC-Pack ODS-A C_{18} column (10 mm × 250 mm, 5 μm). Isocratic elution was performed using water and methanol (75:25, v/v) at a flow rate of 3.5 mL/min and a column temperature of 30 °C, with ultraviolet detection at 280 nm.

Semi-synthesis and HSCCC separation [14]. The reaction conditions were optimized as follows: reaction temperature of 50 °C, reaction duration of 3 h, and a mass ratio of ECG to PPCs of 3:1. A TBE-300C HSCCC system was used for product separation, with a solvent system of *n*-hexane-ethyl acetate-methanol-water (0.2:1.5:0.5:1, v/v/v/v).

A total of 300 mg semi-synthetic products were dissolved in 20 mL of the lower phase of the solvent system and filtered through a 0.45 μm membrane. Separation was carried out in head-to-tail elution mode for 175 min. Eluates were monitored at 280 nm, and fractions were collected manually. Fraction purity was analyzed by ultra-high performance liquid chromatography (UHPLC). Fractions with purity below 90% were further purified by Shimadzu semi-preparative HPLC using a YMC-Pack ODS-A C_{18} column (10 mm × 250 mm, 5 μm). The mobile phase was water–methanol (75:25, v/v) with isocratic elution at 3.5 mL/min and 30 °C, and detection was performed at 280 nm.

2.5 Animals

Male C57BL/6 mice aged 6–8 weeks with a body weight of 22 ± 2 g were supplied by Liaoning Changsheng Biotechnology Co., Ltd., Liaoning, China. All animals were housed under specific pathogen-free (SPF) conditions at Shenyang Pharmaceutical University. The animal experimental protocol was approved by the Animal Ethics Committee of Shenyang Pharmaceutical University (SYPU-IACUC-S2025-0827-102). Mice were kept at 25 °C under a 12 h light/dark cycle, with free access to standard diet and drinking water.

2.6 Grouping of experimental animals and administration of drugs

All mice received one week of adaptive feeding and were randomly divided into four groups with 10 animals per group: control group (CON), DSS model group (DSS), low-dose B2-3′-G group (B2-3′-G_L) and high-dose B2-3′-G group (B2-3′-G_H). Mice in the CON and DSS groups were given normal saline by oral gavage once daily for 14 consecutive days. Animals in the B2-3′-G_L and B2-3′-G_H groups were administered 60 mg/kg and 120 mg/kg B2-3′-G via oral gavage

daily for 14 days, respectively. Starting on the 8th day of administration, mice in the DSS group and two B2-3′-G treatment groups were given 3% (w/v) DSS in drinking water for 7 days to establish colitis models. Body weight, stool characteristics and fecal occult blood were recorded daily throughout the experiment. All mice were anesthetized and euthanized on the 15th experimental day.

2.7 Collection and processing of tissue samples

Colon tissues were isolated, and colon length was measured immediately. Partial colon samples were fixed for histopathological examination, and the remaining tissues were stored at -80 ℃ for subsequent biochemical detection. Spleens were weighed to calculate the spleen index.

2.8 Measurement of body weight and spleen indices

Body weight of each mouse was recorded every day during the experiment. Spleen weight was measured after animal euthanasia, and the spleen index was calculated according to the following formula: spleen index = [spleen weight (g) / body weight (g)] × 100%.

2.9 Assessment of disease activity index (DAI)

Fecal status, body weight changes and fecal occult blood were recorded daily during DSS modeling. Fecal occult blood was detected using commercial kits. The DAI was evaluated based on a previously reported method with minor modifications [15]. The detailed DAI scoring standards are presented in Table 1.

Table 1 Disease activity index score

Score	Weight loss/%	Feces	Faecal occult blood
4	>15%	Diarrhoea	Gross bleeding
3	10%-15%	Thin liquidy stools	Initially blue-brown, gradually dark brown
2	5%-10%	Mucus-like stools	Light green at first, fading to blue-brown
1	1%-5%	Soft stools	Fades from light green to green after 10 s
0	0	Normal	Negative

2.10 H&E staining

Distal colon tissues were fixed in 4% paraformaldehyde for 24 h. After paraffin embedding, tissue blocks were cut into 5 μm-thick sections. Sections were deparaffinized and stained with H&E. Histopathological changes were observed under a light microscope.

2.11 AB-PAS staining

Distal colon tissues were fixed in 4% paraformaldehyde for 24 h and embedded in paraffin. Tissue sections were deparaffinized and rehydrated. Sections were stained with Alcian Blue solution (pH 2.5) for 15-30 min and rinsed with distilled water. After oxidation with periodic acid solution for 5-10 min, sections were incubated with Schiff reagent for 10-20 min. All sections were rinsed with running water, dehydrated and mounted. Histological features were observed under a light microscope.

2.12 Statistical analysis

All data are presented as mean ± standard error of the mean (SEM). Statistical analysis was performed using GraphPad Prism 10.1.2. The Shapiro-Wilk test was used for normality analysis, and the Brown-Forsythe test was applied to evaluate variance homogeneity. For multiple group comparisons, one-way analysis of variance (ANOVA) followed by Tukey's post-hoc test was adopted for data with normal distribution and equal variance. A P value less than 0.05 was defined as statistically significant.

3 Results

3.1 Comprehensive evaluation of three preparation methods for B2-3'-G

Three different reaction systems were established for B2-3′-G synthesis, and each protocol was verified in three independent parallel experiments to confirm stability. The yield and purity of products obtained from each system are summarized below. In the L-cysteine-mediated nucleophilic degradation system, the mass ratio of Cys to PPCs was 3:1, the reaction temperature was 75 ℃, and the reaction duration was 3 h. After purification, the yield of B2-3′-G reached 8.29 mg/g (calculated based on PPCs), with a purity higher than 95.0%. For the acid-catalysed semi-synthesis system, reactions were performed at 55 °C for 1.5 h with an ECG/PPCs mass ratio of 3:1. After semi-preparative HPLC purification, the yield of B2-3′-G was 231.90 mg/g (based on PPCs), and the product purity exceeded 95.0% with good reproducibility. In the semi-synthetic system combined with HSCCC separation, reactions were carried out at 50 °C for 3 h with an ECG/PPCs ratio of 3:1. Reaction products were separated by HSCCC using *n*-hexane-ethyl acetate-methanol-water (0.2:1.5:0.5:1, v/v/v/v) in head-tail elution mode. The final yield of B2-3′-G was 303.00 mg/g (based on PPCs), and the purity reached 98.0%.

L-cysteine containing thiol groups acts as a nucleophile in PPC degradation. L-cysteine (Cys), which contains a thiol group (-SH), is used as a nucleophile. Under citric acid catalysis, carbocations generated from PPCs degradation are captured by Cys to form stable C4 sulfide bonds in the product. The involvement of Cys terminates the continuous degradation of PPCs and retains B2-3′-G in reaction products. This method achieves enrichment of endogenous B2-3′-G in natural PPCs by selectively terminating the degradation reactions.

ECG, a galloylated flavanol monomer, serves as the nucleophile in ECG-based semi-synthesis. Under hydrochloric acid catalysis, PPC cleavage produces carbocations, which are captured by ECG. A new C4-C8 bond forms between the C8 site on the A ring of ECG and PPC-derived carbocations, and the chain reaction is terminated to generate the EC-ECG dimer B2-3′-G.

The semi-synthesis combined with HSCCC is an optimized approach derived from the ECG semi-synthesis method. Both methods share the same mechanism: hydrochloric acid promotes PPC cleavage to produce carbocations, and ECG functions as the exclusive nucleophile. The major improvement lies in optimized reaction parameters and additional HSCCC separation, which enables large-scale acquisition of high-purity target compounds.

In conclusion, the ECG-mediated acid-catalyzed semi-synthesis method dramatically improves B2-3′-G yield compared with L-cysteine-induced partial degradation, with yield increasing from 8.29 mg/g to 231.90-303.00 mg/g. Combination with HSCCC purification further elevates product purity above 98.0%. This integrated protocol is efficient and feasible for large-scale preparation of B2-3′-G.

3.2 Effect of B2-3'-G on body weight of colitis mice

A 3% DSS solution was used to establish a mouse UC model, and B2-3′-G was administrated via oral gavage in treatment groups. The detailed experimental schedule is shown in Fig. 1.

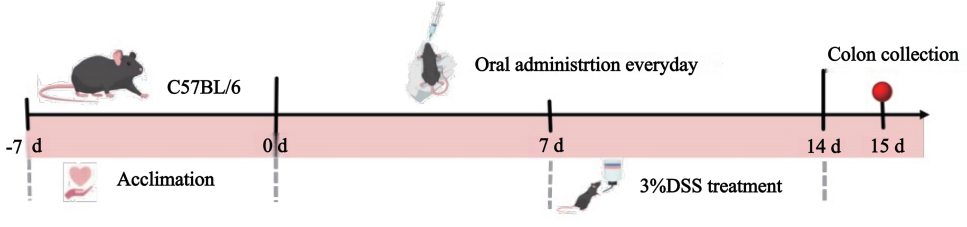
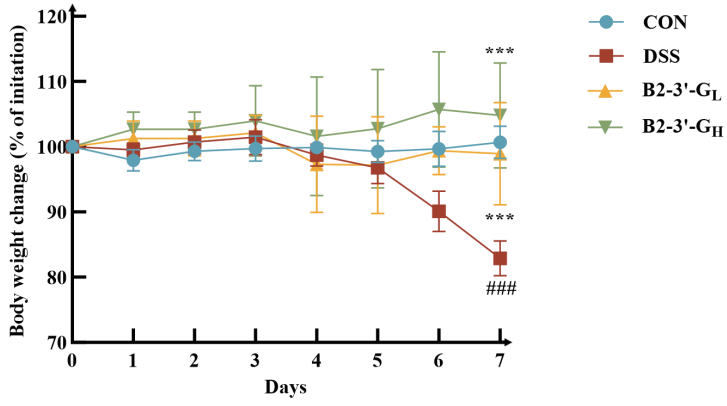


Fig. 1 Schematic of the animal experimental procedure

Mice in the CON group maintained normal food and water intake throughout the experiment, with good mental status, glossy fur and steady weight gain. Mice in the DSS group exhibited decreased food and water intake, lethargy and dull fur starting from the third day after DSS administration. As shown in Fig. 2, obvious body weight loss was observed in the DSS group from the fourth modeling day. Body weight was significantly lower in the DSS group than in the CON group on the seventh day ($P < 0.001$). Mice in the B2-3′-G_L and B2-3′-G_H groups presented mild reduction in food and water intake but better general conditions and fur status relative to the DSS group. Weight loss was also detected in both treatment groups from the fourth day of DSS induction, while the degree of weight loss was markedly attenuated on the seventh day (both $P < 0.001$ vs. DSS group).

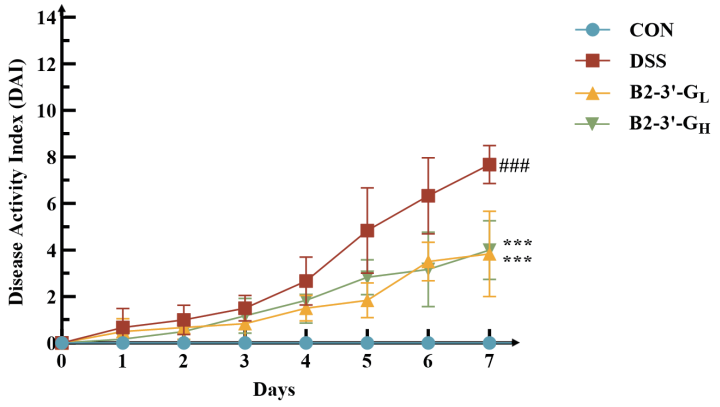
3.3 Effects of B2-3′-G on disease activity index (DAI) of colitis mice

DAI scores were calculated according to body weight loss, fecal consistency and fecal occult blood, and the results are displayed in Fig. 3. DAI scores in the DSS group gradually increased from the third modeling day and were significantly higher than those in the CON group on day 7 ($P < 0.001$). DAI scores of the B2-3′-G_L and B2-3′-G_H groups began to rise on the fourth day. Both low-dose and high-dose B2-3′-G treatments significantly reduced DAI levels on day 7 (both $P < 0.001$ vs. DSS group).



*** $P < 0.05$, ** $P < 0.01$, *** $P < 0.001$ vs. model group; # $P < 0.05$, ## $P < 0.01$, ### $P < 0.001$ vs. control group**

Fig. 2 Effect of B2-3′-G on body weight in colitis mice ($n = 6$)

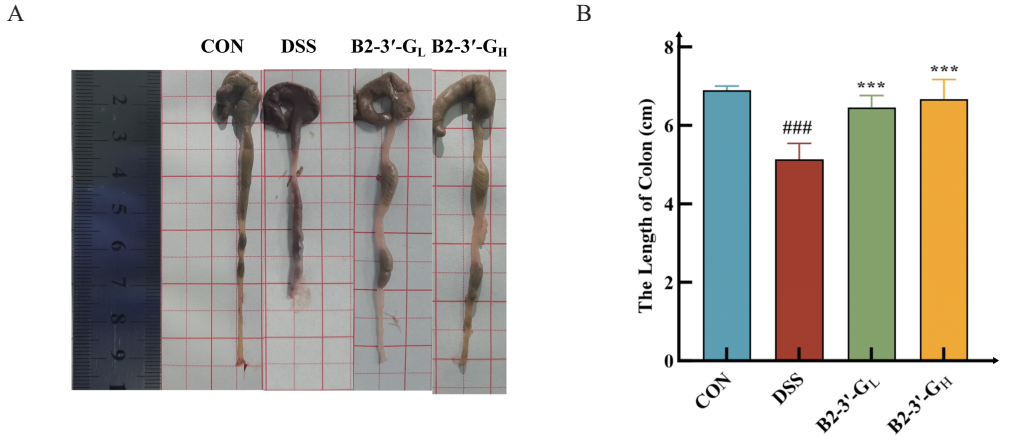


*** $P < 0.05$, ** $P < 0.01$, *** $P < 0.001$ vs. model group; # $P < 0.05$, ## $P < 0.01$, ### $P < 0.001$ vs. control group**

Fig. 3 Effect of B2-3′-G on disease activity index in colitis mice ($n = 6$)

3.4 Effects of B2-3′-G on colon length of colitis mice

Colon shortening is a typical pathological manifestation of DSS-induced colitis. As shown in Fig. 4, colon length was obviously shorter in the DSS group than in the CON group ($P < 0.001$). Administration of B2-3′-G effectively relieved colon shortening. Colon length was significantly restored in the B2-3′-G_L and B2-3′-G_H groups when compared with the DSS group (both $P < 0.001$). These results indicate that B2-3′-G protects colon tissues against DSS-induced damage.

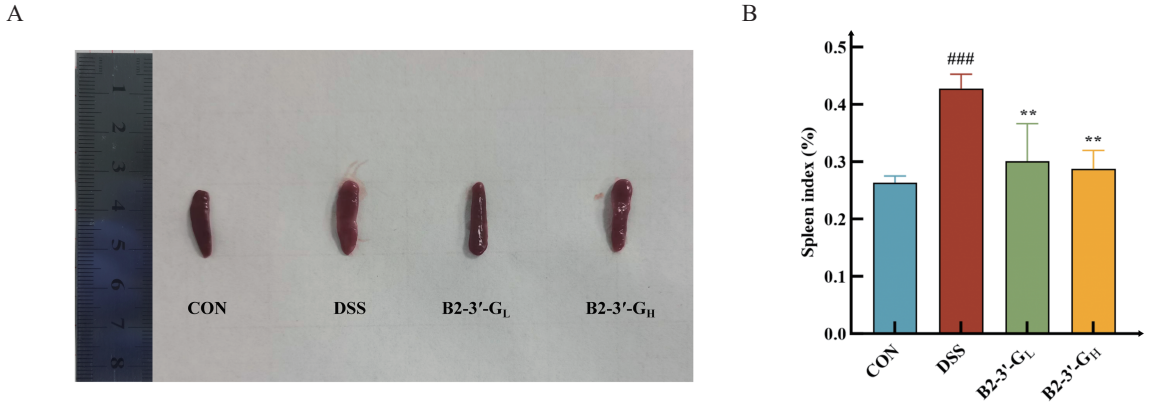


representative photographs (A) and length quantification; (B) of colon tissues; * $P < 0.05$, ** $P < 0.01$, *** $P < 0.001$ vs. model group; # $P < 0.05$, ## $P < 0.01$, ### $P < 0.001$ vs. control group

Fig. 4 Effect of B2-3′-G on colon length in colitis mice ($n = 6$)

3.5 Effects of B2-3′-G on spleen index of colitis mice

Spleen index is a key indicator reflecting systemic inflammatory status. As shown in Fig. 5, the spleen index was significantly elevated in the DSS group relative to the CON group ($P < 0.001$). B2-3′-G treatment reduced spleen enlargement and decreased spleen index. Significant differences were observed between the DSS group and the two B2-3′-G treatment groups (B2-3′-G_L: $P < 0.01$; B2-3′-G_H: $P < 0.05$)



representative photographs of spleen tissue (A) and spleen index; (B) * $P < 0.05$, ** $P < 0.01$, *** $P < 0.001$ vs. model group; # $P < 0.05$, ## $P < 0.01$, ### $P < 0.001$ vs. control group

Fig. 5 Effect of B2-3′-G on spleen index in colitis mice ($n = 6$)

3.6 Effects of B2-3′-G on colon histopathology of colitis mice (H&E staining)

H&E staining revealed severe intestinal damage and structural disorders in DSS-induced UC mice (Fig. 6). Typical lesions included extensive inflammatory cell infiltration, severe destruction of mucosal epithelium, disrupted gland architecture, loss of crypts and depletion of goblet cells and mucin.

B2-3′-G treatment alleviated the above pathological injuries. Reduced inflammatory cell infiltration and milder damage to epithelial and crypt structures were observed in B2-3′-G intervention groups. B2-3′-G effectively alleviates DSS-induced pathological changes in colonic tissue, and its intestinal protective effects may be associated with inflammatory suppression, epithelial repair, and crypt structure maintenance.

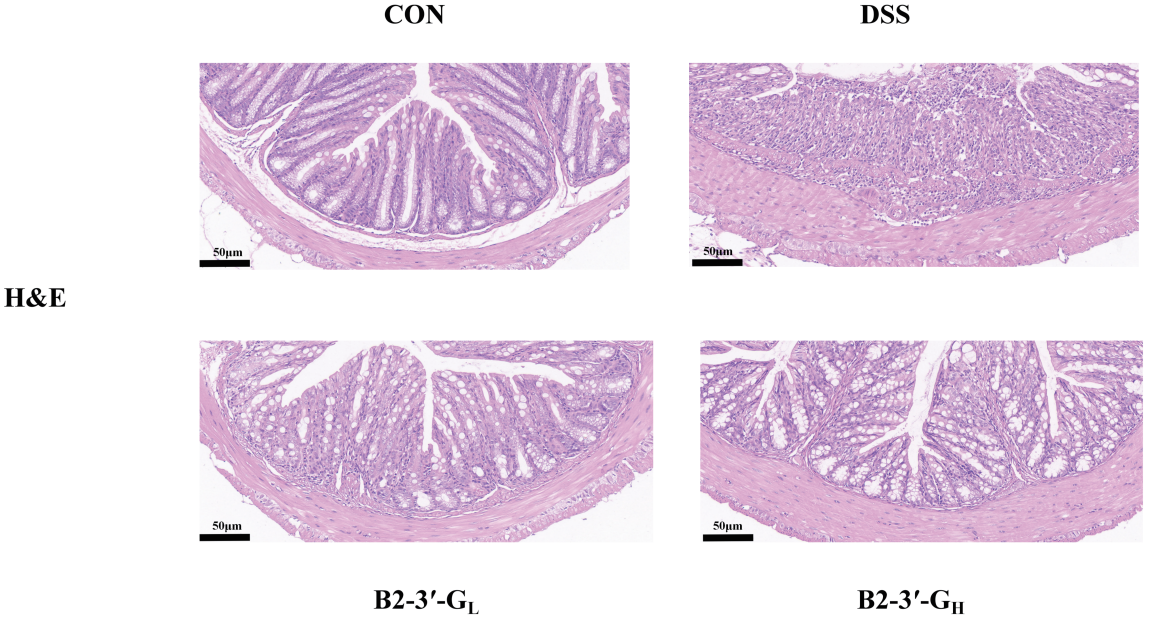


Fig. 6 Effect of B2-3′-G on colon histopathology in colitis mice (× 20)

3.7 Effects of B2-3′-G on goblet cells and mucin secretion of colitis mice (AB-PAS staining)

Goblet cells are specialized secretory cells in intestinal epithelium, which mainly synthesize and secrete mucins such as MUC2 to form the intestinal mucus layer. The mucus layer acts as the first line of intestinal innate immunity. It isolates intestinal epithelium from pathogenic microorganisms and provides a stable microenvironment for commensal bacteria colonization. The quantity and function of goblet cells directly reflect the integrity of the intestinal mucosal barrier.

AB-PAS staining results (Fig. 7) showed that the number of colonic goblet cells decreased sharply in the DSS group. DSS disrupts intestinal epithelial barriers and activates inflammatory responses, which leads to goblet cell loss and mucus layer thinning. This pathological change further aggravates the stimulation of submucosal immune cells by intestinal contents and forms a vicious cycle. B2-3′-G treatment obviously reversed the reduction of goblet cells. The recovery of goblet cell number demonstrates the repairing effect of B2-3′-G on intestinal structure and barrier function, which provides morphological evidence for its application in IBD treatment.

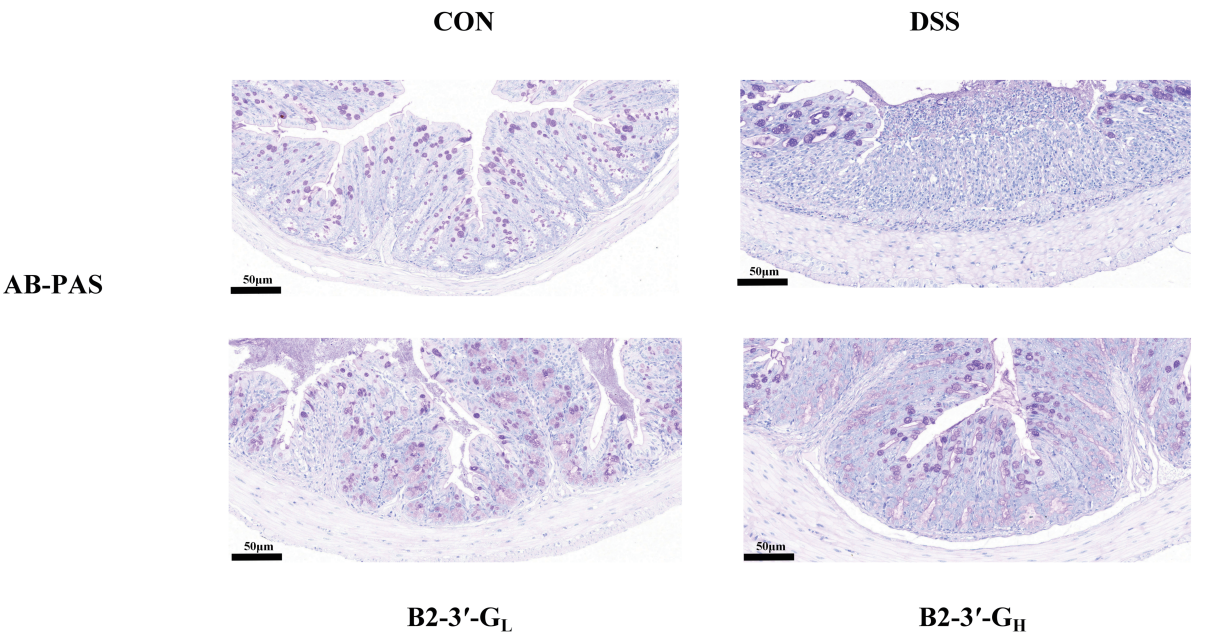


Fig. 7 Effect of B2-3′-G on goblet cells and mucin secretion in colitis mice (× 20)

4 Discussion

Ulcerative colitis (UC) has become a severe global health challenge, and the development of novel effective therapies is urgently needed [16-17]. However, existing clinical drugs are limited by adverse reactions and high recurrence rates; so exploration of new intervention strategies is essential [18]. Multiple studies have confirmed that procyanidins can alleviate DSS-induced colonic damage in animal models of UC [19-20]. Nevertheless, the protective effects of single-component B2-3′-G against UC have not been reported previously. The present study established a DSS-induced UC mouse model and verified for the first time that B2-3′-G effectively alleviates body weight loss, improves DAI scores and mitigates colonic pathological damage.

Although the protective effects of B2-3′-G against DSS-induced UC in mice have been confirmed, the underlying molecular mechanisms remain to be clarified. Future studies will combine transcriptomics and metabolomics to screen potential inflammation-related signaling pathways involved in the anti-colitic effects of B2-3′-G, and relevant cell models will be used for mechanistic validation.

5 Conclusions

This study investigated three different preparation routes for B2-3′-G, with a maximum yield of 303.00 mg/g and product purity above 98.0%. In the DSS-induced UC mouse model, B2-3′-G significantly alleviated body weight loss and colon shortening, reduced DAI scores, and improved histological damage. In summary, B2-3′-G is a promising candidate compound for UC treatment. The present findings provide experimental support and theoretical reference for the development of new therapeutic regimens against UC.

References

[1] Williams T, Ashleigh G, Larbi B, et al. Determinants of IBD Heritability: Genes, Bugs, and More. Inflamm Bowel Dis, 2018, 24 (6): 1133-48.

[2] Michael HW, Oleg S, Hyun SK, et al. US Inflammatory Bowel Disease Prevalence: Surveillance Data from the U.S. National Health and Nutrition Examination Survey.

Prev Med Rep, 2023, 33 (Suppl C): 102173.

[3] Zhang C, Zhang JT, Zhang YL, et al. Identifying neutrophil-associated subtypes in ulcerative colitis and confirming neutrophils promote colitis-associated colorectal cancer. Front Immunol, 2023, 14: 1095098.

[4] Laurie BG, Konstantinos P, Adam SC, et al. Review article: emerging drug therapies in inflammatory bowel disease. Aliment Pharmacol Ther, 2022, 55 (7): 789-804.

[5] Spranger I, Sun BS, Mateus AM, et al. Chemical characterization and antioxidant activities of oligomeric and polymeric procyanidin fractions from grape seeds. Food Chem, 2008, 108: 519-32.

[6] Sachin V, Subhash L, Vishwaraman M, et al. Anti-inflammatory and anti-arthritic activity of type-A procyanidine polyphenols from bark of Cinnamomum zeylanicum in rats. Food Sci Hum Wellness, 2013, 2 (2): 59-67.

[7] Mu JJ, Xu JW, Wang LL, et al. Anti-inflammatory effects of purple sweet potato anthocyanin extract in DSS-induced colitis: modulation of commensal bacteria and attenuated bacterial intestinal infection. Food Funct, 2021, 12 (22): 11503-14.

[8] Ai LY, Ren YM, Zhu MM, et al. Synbindin restrains proinflammatory macrophage activation against microbiota and mucosal inflammation during colitis. Gut, 2021, 70 (12): 2261-72.

[9] Wang R, Dang M, Zhu W, et al. Galloyl group in b-type proanthocyanidin dimers was responsible for its differential inhibitory activity on 3T3-L1 preadipocytes due to the strong lipid raft-perturbing potency. J Agric Food Chem, 2021, 69 (17), 5216-25.

[10] Luo L, Bai R, Zhao Y, et al. Protective effect of grape seed procyanidins against H_2O_2-induced oxidative stress in PC-12 neuroblastoma cells: structure-activity relationships. Food Sci, 2018, 83 (10), 2622-8.

[11] Zhang ST, Li LX, Cui Y, et al. Preparative high-speed counter-current chromatography separation of grape seed proanthocyanidins according to degree of polymerization. Food Chem, 2017, 219: 399-407.

[12] Yu YX, Zuo CY, Li MR, et al. Novel l-Cysteine Incomplete Degradation Method for Preparation of Procyanidin B2-3′-O-Gallate and Exploration of its in Vitro Anti-inflammatory Activity and in Vivo Tissue Distribution. J Agric Food Chem, 2024, 72 (8): 4023-34.

[13] Zhang ST, Wang F, Yu YX, et al. Procyanidin B2-3′-O-Gallate Derived from Grape Seed Polymeric Procyanidins via the Galloyl-Attached Nucleophilic Degradation as a Potential Hepatoprotective Agent. J Agric Food Chem, 2024, 72 (34): 18918-29.

[14] Yu YX, Sun MY, Han PY, et al. Large-Scale Semisynthesis of Bioactive Procyanidin B2 3,3′-di-O-gallate: Structural Characterization, Simulated In Vitro Digestion, and Protective Effects against Colitis. J Agric Food Chem, 2026, 74 (6): 5304-17.

[15] Yong F, Oluf P. Gut microbiota in human metabolic health and disease. Nat Rev Microbiol, 2021, 19 (1): 55-71.

[16] Pan YS, Bharati K. Ulcerative colitis, frailty, and beyond. Expert Rev Gastroenterol Hepatol, 2026, 20 (4): 303-11.

[17] Samara MD, Karen Z. Ulcerative Colitis. Surg Clin North Am, 2026, 106 (1): 121-32.

[18] Roda G, Ng SC, Kotze PG, et al. Publisher Correction: Crohn's disease. Nat Rev Dis Primers, 2020, 6 (1): 26.

[19] Guo XX, Xu Y, Geng RX, et al. Curcumin Alleviates Dextran Sulfate Sodium-Induced Colitis in Mice Through Regulating Gut Microbiota. Mol Nutr Food Res, 2022, 66 (8): e2100943.

[20] Sheng KL, Zhang GH, Sun M, et al. Grape seed proanthocyanidin extract ameliorates dextran sulfate sodium-induced colitis through intestinal barrier improvement, oxidative stress reduction, and inflammatory cytokines and gut microbiota modulation. Food Funct, 2020, 11 (9): 7817-29.